

the fractionation of Pb and U during fluid transport is even larger than suggested by the data in Table 1.

In equilibrium with clinopyroxene and other minerals such as olivine and orthopyroxene, Sr partitions in favour of a hydrous chloridic fluid (Table 1). This provides a mechanism that allows contamination of the Sr isotopes in the zone of melting by Sr from the subducted oceanic slab, in agreement with the relatively radiogenic Sr-isotope composition of many calc-alkaline magmas^{4,6,7}. Another distinctive feature of such magmas are often radioactive disequilibria²² with strong enrichments of ²²⁶Ra over ²³⁰Th. These disequilibria may also be a result of fluid transport. Radium behaves geochemically very similar to Ba. From the data in Table 1, one would therefore expect that a hydrous chloridic fluid would strongly enrich ²²⁶Ra over ²³⁰Th, as is observed¹⁹.

From the foregoing discussion, it appears that the entire trace-element enrichment pattern in calc-alkaline magmas could be explained by metasomatism involving an alkali-chloride-rich fluid. This would imply that ultimately the trace element composition of the continental crust is largely a result of the complexing properties of chloride in supercritical aqueous solutions. Because the composition of the fluid released in the subducted slab depends on the composition of the sea water the oceanic crust had been reacting with, very old calc-alkaline rocks may preserve a record of the chemical evolution of sea water. The development of the typical modern trace element signature in subduction-zone vol-

canics may mark the point in geological history when sea water approached its modern composition, rather than reflecting a change in the style of global tectonics. □

Received 3 July 1995; accepted 1 February 1996.

1. Davies, J. H. & Stevenson, D. J. *J. geophys. Res.* **97**, 2037–2070 (1992).
2. Tatsumi, Y., Hamilton, D. L. & Nesbitt, R. W. *J. Volcan. geotherm. Res.* **29**, 293–309 (1986).
3. Maury, R. C., Defant, M. J. & Joron, J. L. *Nature* **360**, 661–663 (1992).
4. Hawkesworth, C. J., Gallagher, K., Hergt, J. M. & McDermott, F. *Lithos* **33**, 169–188 (1994).
5. Miller, D. M., Goldstein, S. L. & Langmuir, C. H. *Nature* **368**, 514–520 (1994).
6. Perfit, M. R., Gust, D. A., Bence, A. E., Arculus, R. J. & Taylor, S. R. *Chem. Geol.* **30**, 227–256 (1980).
7. Arculus, R. J. *Lithos* **33**, 189–208 (1994).
8. Philippot, P. *Chem. Geol.* **108**, 93–112 (1993).
9. Brenan, J. M. & Watson, E. B. *Earth planet. Sci. Lett.* **107**, 672–688 (1991).
10. Keppler, H. & Wyllie, P. J. *Contr. Miner. Petrol.* **109**, 139–150 (1991).
11. Huheey, J. E. *Inorganic Chemistry* (Harper & Row, New York, 1983).
12. Brenan, J. M., Shaw, H. F., Ryerson, F. J. & Phinney, D. L. *Geochim. cosmochim. Acta* **59**, 3331–3350 (1995).
13. Johnson, K. T. M. & Kinzler, R. J. *Eos* (abstr.) **70**, 1388 (1989).
14. Chaussidon, M. & Libourel, G. *Geochim. cosmochim. Acta* **57**, 5053–5062 (1993).
15. Carroll, M. R. & Wyllie, P. J. *Am. Mineral.* **75**, 345–357 (1990).
16. McCulloch, M. T. & Gamble, J. A. *Earth planet. Sci. Lett.* **102**, 358–374 (1991).
17. Hofmann, A. E. *Earth planet. Sci. Lett.* **90**, 297–314 (1988).
18. Ayers, J. C. & Eggler, D. H. *Geochim. cosmochim. Acta* **59**, 4237–4246 (1995).
19. Condomines, M., Hemond, C. & Allègre, C. J. *Earth planet. Sci. Lett.* **90**, 243–262 (1988).
20. Hart, S. R. & Dunn, T. *Contr. Miner. Petrol.* **113**, 1–8 (1993).
21. Irving, A. J. *Geochim. cosmochim. Acta* **42**, 743–770 (1978).
22. Green, T. H. *Chem. Geol.* **117**, 1–36 (1994).

ACKNOWLEDGEMENTS. I thank A. Dietel for carrying out all ICP-analyses reported here and D. Krausse for his assistance with the electron microprobe. A review by T. Plank improved the manuscript. This work was supported by the German Science Foundation (DFG).

The rock–paper–scissors game and the evolution of alternative male strategies

B. Sinervo & C. M. Lively

Department of Biology and Center for the Integrative Study of Animal Behavior, Indiana University, Bloomington, Indiana 47405, USA

MANY species exhibit colour polymorphisms associated with alternative male reproductive strategies, including territorial males and ‘sneaker males’ that behave and look like females^{1–3}. The prevalence of multiple morphs is a challenge to evolutionary theory because a single strategy should prevail unless morphs have exactly equal fitness^{4,5} or a fitness advantage when rare^{6,7}. We report here the application of an evolutionary stable strategy model to a three-morph mating system in the side-blotched lizard. Using parameter estimates from field data, the model predicted oscillations in morph frequency, and the frequencies of the three male morphs were found to oscillate over a six-year period in the field. The fitnesses of each morph relative to other morphs were non-transitive in that each morph could invade another morph when rare, but was itself invadable by another morph when common. Concordance between frequency-dependent selection and the among-year changes in morph fitnesses suggest that male interactions drive a dynamic ‘rock–paper–scissors’ game⁷.

From 1990–95, we studied territory use and patterns of sexual selection on male side-blotched lizards (*Uta stansburiana*), a small territorial iguanid lizard (3–10 g) that matures in one year in the inner Coast Range of California (Merced County). Territory defence by males is dependent on a throat-colour polymorphism that develops as males mature (Fig. 1). Males with orange throats are very aggressive and defend large territories. Males with dark blue throats are less aggressive and defend smaller territories. Males with prominent yellow stripes on their throats are ‘sneakers’ and do not defend territories (receptive females also have yellow-striped throats). Aggression in orange males is linked to higher levels of testosterone⁸, as is the case for other vertebrates^{3,9–12}.

Male fitness was estimated by the number of females that are exclusively on his home range (monopolized females), plus his share of females (shared females) that overlap with the home range of other males (Fig. 3a–e). Significant changes in morph frequency among years were consistent with an evolutionary response to sexual selection (Fig. 3), particularly in light of the heritability ($h^2 = 0.96$) for throat colour in nature (Fig. 2). Fitness regression coefficients¹³ describe the impact that neighbouring morphs have on male fitness. ‘Local’ frequency-dependent sexual selection among morphs could drive frequency fluctuations among years (Fig. 3). The population cycled from high frequency of blue (1991), to high frequency of orange (1992) to high frequency of yellow (1993–94) and returned to high frequency of blue (1995).

Orange males increased from 1991 to 1992, owing to their significantly higher monopoly on females in 1991 (Fig. 3a). Moreover, the decline in blue males from 1991 to 1994 arose from losses to adjacent orange males. In 1992, blue males lost a monopoly on 0.11 ($P < 0.05$) females for every orange neighbour (0.59 oranges on average). Conversely, in 1993 orange males gained a monopoly on 1.10 females ($P < 0.01$) for each blue neighbour (0.09 blues on average). After peaking in 1992, orange males declined in frequency from 1992 to 1995, and their decline was consistent with a drop in monopolization observed for orange males (Fig. 3a, b).

Although no morph had a clear fitness advantage in 1992 or 1993, the decline in orange males was coincident with an increase in the frequency of yellow males (Fig. 3c, d). Losses of orange males were directly related to the number of neighbouring yellows. In 1992, each orange neighbour increased a yellow male’s monopoly by 0.23 females ($P < 0.0001$) and a yellow male’s share by 0.54 females ($P < 0.0001$, 0.46 oranges on average). Conversely, in 1995 orange males lost a share of 0.55 females ($P < 0.01$) to each yellow neighbour (2.25 yellows on average).

Yellow males declined in frequency from 1993 to 1995, and their decline was due in part to lower monopolization of female home ranges by yellow males compared to blue or orange males (Fig. 3d). In addition, each blue male obtained 0.25 shared females ($P < 0.01$) for each yellow neighbour (0.63 yellows on average). In 1995, the profile of selection returns to the pattern observed in 1991, when orange males have high rates of female monopoly (compare Fig. 3e with a), and orange males should

FIG. 1 Colour polymorphisms of male side-blotched lizards. Males with orange throats (lower left panel) and/or sides (male with orange flank on the left, top panel) are 'ultra dominant' to males with blue on their throat (lower centre panel, and male on the right, top panel). Males with yellow throats (lower right panel) resemble females in morphology in that females have yellow throats when receptive. Whereas males with orange, blue and yellow throats represent discrete and unambiguous colour scores (orange, 2; blue, 1; yellow, 0) a small fraction of 'hybrid' blue males mature with dark blue throats and very thin orange stripes. These males were categorized as blue based on behaviour, and given a colour score of 1.5 for the heritability analyses. Likewise a small fraction of yellow-throated males mature with yellow throats with very pale blue stripes (not dark blue) and these males were categorized as yellow and given a colour score of 0.5 for the heritability analyses.

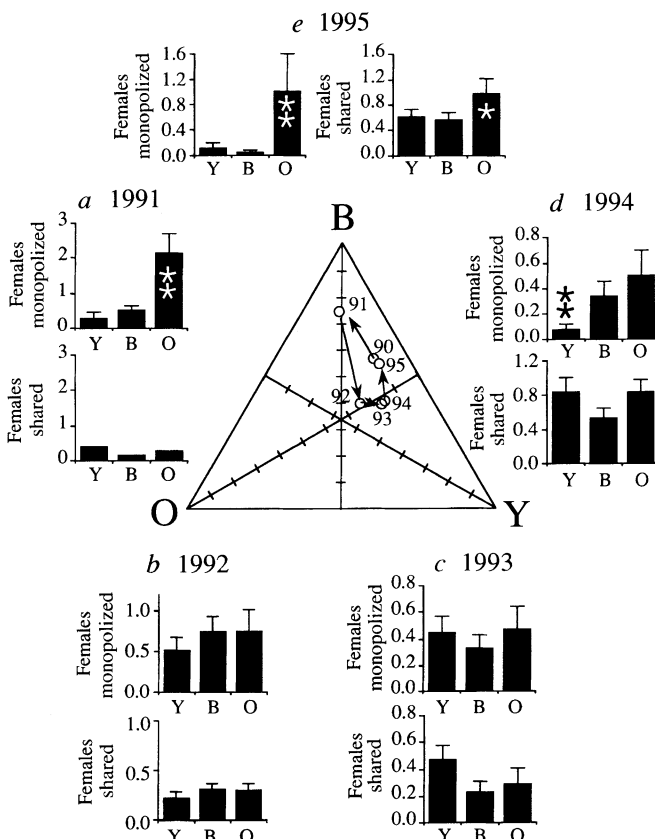
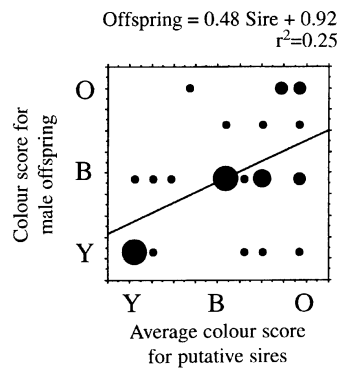


FIG. 2 During 1990–95, significant among-year changes in the frequency of adult male colour polymorphisms (Fig. 1) on a 250-m-long sandstone outcropping (central triangle, Chi-square, $P < 0.01$) were consistent with significant variation in sexual selection (histograms a–e, number of females on a male's territory, $\bar{x} \pm \text{s.e.}$), and morph fitness (see text). Frequency of morphs are plotted for each year as follows: 0–100% blue from base to apex, 0–100% orange from right side to left vertex, and 0–100% yellow from left side to right vertex.

METHODS. A male monopolized a female if he was the only male observed on a female's home range. We partitioned females with many males on her home range among males (a mean which differs from 2 means is denoted by **, and * denotes a mean that differs from a single mean; Fisher's LSD post-hoc test, $P < 0.05$). Survival which is based on comprehensive monthly recaptures¹⁵, reproductive success^{15–17}, and territorial behaviour (discriminated with a dorsal paint-mark)^{14,15} of all uniquely marked adults was followed. Home ranges were mapped^{14,15} from daily visual censuses ($N_{\text{males}} = 62, 127, 105, 116, 74$; $N_{\text{females}} = 133, 189, 178, 140, 106$. $N_{\text{sightings}} = 518, 1,846, 1,791, 3,466, 1,664$ for 1991–95, respectively). Only females that survived to produce eggs were considered. Eggs were collected from all females and offspring were released upon hatching^{15–17}. Survival of uniquely marked offspring was censused at maturity the next year¹⁴.

FIG. 3 Heritability ($h^2 = 0.96$) of male throat colouration for animals in nature. Maternity of offspring on the site was known with certainty¹⁸. Eggs were obtained from uniquely marked females and their uniquely marked offspring were released randomly with respect to sibship back on site when they hatch^{14,18}. Throat colour of surviving male offspring was scored at maturity (Fig. 1). We assumed that a monopolizing male is the only sire of a dam's offspring. In cases of shared females, probability of paternity was assumed to be proportional to a putative sire's access to the dam. Regression of offspring and 'sire's' throat score yields $h^2 = 0.96$. Quantitative genetic analysis assumes many autosomal loci¹⁹, however, one or two loci may govern colour.



increase in 1996. However, given that each orange male lost a share of 0.55 females to each yellow neighbour (see above), we also predict that yellows should 'hitchhike a fitness ride' from oranges and increase in frequency relative to blues, as in 1991.

The pattern of frequency-dependent sexual selection among years leads to a key prediction: when a morph reaches a low frequency, it should produce the most mature offspring in the next year (for example, at the 'vertices' of the cycle, Fig. 3). Indeed, analysis of fitness, as measured by survival of offspring from putative sires, showed a significant morph \times year interaction ($P < 0.0001$, morph fitness, $W_i = W_{i=rare}/W_{i=common}$). In 1991, orange males produced the most offspring that survived to the next year ($W_o = 4.73$, $W_b = 1.00$, $W_y = 1.61$), yellow males produced the most in 1992 ($W_o = 1.28$, $W_b = 1.00$, $W_y = 1.45$), and blue males produced the most in 1994 ($W_o = 0.90$, $W_b = 1.26$, $W_y = 1.00$). Differences in fitness of putative sires were consistent with sexual selection (above) and were not due to survival differences of offspring to maturity ($P > 0.36$, $N = 1, 202$).

We estimated the frequency-dependent 'fitness payoffs' of a

rare morph competing against a common morph⁷ from the 'local' frequency-dependent interactions among males (Fig. 4). The fitness of a rare i^{th} strategy against a common (j^{th}) strategy was estimated as:

$$W_{ij} = [M_i + N_i \times G_{M_{ij}}] + [S_j + N_j \times G_{S_{ij}}] \quad (1)$$

where fitness, W_{ij} , is the sum of two linear equations. The linear equation in the left brackets is fitness acquired through monopoly of female territories, M_i , adjusted by $G_{M_{ij}}$ which is the slope of the line (partial regression coefficients, above) describing gains and losses for the i^{th} strategy for each neighbour of the j^{th} strategy. The number of neighbours, N_i , is a phenotypic trait of the i^{th} strategy. N_i describes the total number of males that the i^{th} strategy is playing against ($N_y = 5.03$, $N_b = 2.35$ and $N_o = 2.95$ from 1991–95). This assumes gains and losses are linearly related to the number of neighbouring males. Likewise, fitness from shared access to females, S_j , is also adjusted by $G_{S_{ij}}$ and N_j . Equation (1) can be written in a compact matrix form where, W , is a pay-off matrix (Fig. 4a) that describes the relative fitness of each rare morph in competition with a common morph (elements $i = 1, 2$, and 3 of W correspond to strategies y, b, and o):

$$W = M + S + N \cdot (G_M + G_S) \quad (2)$$

When the rare and common morph are the same strategy, they have equal fitness (diagonal elements of W are equal to 1.0, Fig. 4a). To be an evolutionary stable strategy (ESS), a morph must have higher fitness than the other morphs when it is both rare and common. It is clear that no morph is an ESS (Fig. 4). When generations are discrete, the population may be expected to oscillate around an 'attractor'. Assuming $h^2 = 1$, the frequency of the i^{th} morph in the next generation, $p_{i,t+1}$, can be written as⁶:

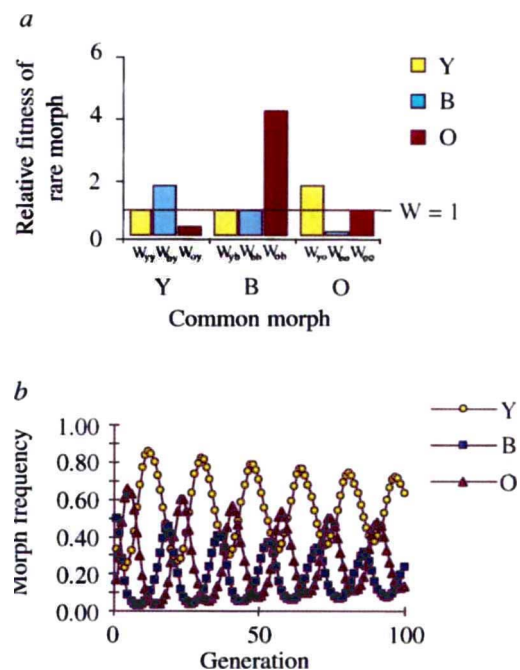
$$p_{i,t+1} = p_{i,t} \left(\frac{W_{i,t}}{\bar{W}} \right) \quad (3)$$

where $W_{i,t} = p_{1,t}W_{i1} + p_{2,t}W_{i2} + p_{3,t}W_{i3}$ (where W_{i1} , W_{i2} , and W_{i3} are elements of W , equation (2)), and $\bar{W} = \sum p_{i,t} \times W_{i,t}$. Iterations of the model using parameter estimates from field data, give oscillations qualitatively similar (Fig. 4b) to those observed in the field (Fig. 2). The model also shows that no morph is an ESS, which

FIG. 4 a, The pay-off matrix of a rare yellow, blue or orange strategy playing against each strategy when common. The strategy (yellow) is an ESS if it cannot be invaded when common by either a rare orange or a rare blue strategy: $W_{yy} > W_{oy}$, and $W_{yy} > W_{by}$. Similarly, blue is an ESS if $W_{bb} > W_{ob}$, and $W_{bb} > W_{yb}$; and orange is an ESS if $W_{oo} > W_{yo}$, and $W_{oo} > W_{bo}$. It is clear that every morph is invadable by one other morph and thus no morph is an ESS. Analysis of the pay-off matrix, W , was partitioned according to access to monopolized and shared females (equation (2) and Fig. 2). We observed significant frequency-dependence in every year (see text). Partial regression coefficients (adjusted to relative fitness) describing gains and losses are given by:

$$N(G_M + G_S) = \begin{bmatrix} 5.03 & 0 & 0 \\ 0 & 2.35 & 0 \\ 0 & 0 & 2.95 \end{bmatrix} \times \left(\begin{bmatrix} 0 & 0 & +0.15 \\ 0 & 0 & -0.07 \\ 0 & 1.24 & 0 \end{bmatrix} + \begin{bmatrix} 0 & 0 & +0.35 \\ +0.27 & 0 & 0 \\ -0.93 & 0 & 0 \end{bmatrix} \right)$$

For example, a rare yellow would gain 0.15 females by monopoly and 0.35 females by sharing when playing against common orange males. A rare yellow's gains in relative fitness are equal to $5.03 \times (0.15 + 0.35)$, given 5.03 orange neighbours for the rare yellow. Fitness gains and losses between rare and common neighbours, $N(G_M + G_S)$, are used to adjust relative fitness of each morph (for example, female monopoly and shares, Fig. 2). b, The empirically derived pay-off matrix, W , was used in a simple quantitative genetic model (equation (3)). The model predicts cycles in morph frequency with a period of 12 years. Although the magnitude of oscillations appears to damp over time, any random perturbation of frequency will renew the strength of the oscillations.



leads to dynamic oscillations in frequency (Fig. 4b). Oscillations in morph frequency (not shown) are surprisingly robust in an age-structured model that includes small, but significant differences in yearly adult survival between morphs ($l_y = 0.167$, ($N = 209$), $l_b = 0.136$ ($N = 199$), and $l_o = 0.048$ ($N = 84$), Chi-square: l_o versus l_y , $P < 0.01$, l_o versus l_b , $P = 0.05$, l_y versus l_b , n.s.):

$$p_{i,t+1} = [l_i \times p_{i,t}] + (1 - l_{\text{adult}}) \times p_{i,t} \left(\frac{W_{i,t}}{\bar{W}} \right) \quad (4)$$

where, $p_{i,t+1}$ is determined by the probability of adult morph survival to the next year (l_i) and relative fitness of each morph (equation (3)) is adjusted by the proportion of new recruits in the

next year, which is approximated by $(1 - l_{\text{adult}}) = 1 - \sum p_{i,t} \times l_i$, or one minus average adult survival.

We have described the first biological example of a cyclical 'Rock-paper-scissors' game⁷. As in the game where paper beats rock, scissors beat paper, and rock beats scissors, the wide-ranging 'ultradominant' strategy of orange males is defeated by the 'sneaker' strategy of yellow males, which in turn defeated by the mate-guarding strategy of blue males; the orange strategy defeats the blue strategy to complete the dynamic cycle. Frequency-dependent selection maintains substantial genetic variation in alternative male strategies, while at the same time prohibiting a stable equilibrium in morph frequency. □

Received 31 October 1995; accepted 18 January 1996.

- Gross, M. R. *Phil. Trans. R. Soc. B* **332**, 59–66 (1991).
- Moore, M. C. & Thompson, C. W. in *Progress in Clinical and Biological Research* (eds Epple, A., Scanes, C. G. & Stetson, M. H.) 685–690 (1990).
- Brantley, R. K., Wingfield, J. C. & Bass, A. H. *Horm. Behav.* **27**, 332–347 (1993).
- Ryan, M. J., Pease, C. M. & Morris, M. R. *Am. Nat.* **139**, 21–31 (1992).
- Shuster, S. M. & Wade, M. J. *Nature* **350**, 608–610 (1991).
- Chamov, E. L. *Life History Invariants: Some Explorations of Symmetry in Evolutionary Ecology* 1–167 (Oxford Univ. Press, New York, 1993).
- Maynard-Smith, J. *Evolution and the Theory of Games* (Cambridge Univ. Press, Cambridge, 1982).
- Sinervo, B., Miles, D. B., DeNardo, D., Frankino, T. & Klukowski, M. *Proc. R. Soc. Lond.* (submitted).
- Kindler, P. M., Phillip, D. P., Gross, M. R. & Bahr, J. M. *Gen. comp. Endocrinol.* **75**, 446–453 (1989).

- Rand, M. S. *Gen. comp. Endocrinol.* **88**, 461–468 (1992).
- Cardwell, J. R. & Liley, N. R. *Gen. comp. Endocrinol.* **81**, 7–20 (1991).
- Hews, D. K., Knapp, R. & Moore, M. C. *Horm. Behav.* **28**, 96–115 (1994).
- Lande, R. & Arnold, S. J. *Evolution* **37**, 1210–1226 (1983).
- Sinervo, B., Doughty, P., Huey, R. B. & Zamudio, K. *Science* **258**, 1927–1930 (1992).
- Sinervo, B. & DeNardo, D. F. *Evolution* (in the press).
- DeNardo, D. F. & Sinervo, B. *Horm. Behav.* **28**, 53–65 (1994).
- DeNardo, D. F. & Sinervo, B. *Horm. Behav.* **28**, 273–287 (1994).
- Sinervo, B. & Doughty, P. *Evolution* (in the press).
- Falconer, D. S. *Introduction to Quantitative Genetics* 1–340 (Longman, New York, 1981).

ACKNOWLEDGEMENTS. We thank P. Stadler and R. Schrimp for permission to work on their land. This research was supported by NSF grants to B.S. and C.M.L. Video segments of morph head-bob patterns can be obtained in Quick Time format through the World Wide Web (<http://sunflower.bio.indiana.edu/~bsinervo>).

A role for melanin-concentrating hormone in the central regulation of feeding behaviour

Daqing Qu, David S. Ludwig*, Steen Gammeltoft†, Mary Ann Pelleymounter‡, Mary Jane Cullen‡, Wendy Foulds Mathes§, Jeanne Przypek§, Robin Kanarek§ & Eleftheria Maratos-Flier||

Elliott P. Joslin Research Laboratory, Joslin Diabetes Center, and Department of Medicine, Brigham and Women's Hospital, Boston, Massachusetts 02215, USA

* Department of Medicine, Division of Endocrinology, Beth Israel Hospital, Boston, Massachusetts 02215, USA

‡ Department of Neurobiology, Amgen Inc., 1840 DeHavilland Drive, Thousand Oaks, California 91320, USA

§ Department of Psychology, Tufts University, Medford, Massachusetts 02155, USA

THE hypothalamus plays a central role in the integrated regulation of energy homeostasis and body weight, and a number of hypothalamic neuropeptides, such as neuropeptide Y (ref. 1), galanin², CRH (ref. 3), and GLP-1 (ref. 4), have been implicated in the mediation of these effects. To discover new hypothalamic peptides involved in the regulation of body weight, we used differential display polymerase chain reaction⁵ to identify messenger RNAs that are differentially expressed in the hypothalamus of *ob/+* compared with *ob/ob* C57Bl/6J mice. We show here that one mRNA that is overexpressed in the hypothalamus of *ob/ob* mice encodes the neuropeptide melanin-concentrating hormone (MCH). Fasting further increased expression of MCH mRNA in both normal and obese animals. Neurons containing MCH are located in the zona incerta and in the lateral hypo-

thalamus. These areas are involved in regulation of ingestive behaviour, but the role of MCH in mammalian physiology is unknown. To determine whether MCH is involved in the regulation of feeding, we injected MCH into the lateral ventricles of rats and found that their food consumption increased. These findings suggest that MCH participates in the hypothalamic regulation of body weight.

Using differential display polymerase chain reaction (PCR) with 180 primer pairs, we screened 30% of expressed mRNAs. Fifty-two DNA bands appeared to be differentially expressed. Of 35 bands further evaluated using northern blot analysis with riboprobes, no signal could be detected for 9 bands, and no difference in expression was observed in 20 bands. Thus, of about 9,000 complementary DNAs screened, differences in expression were confirmed for only six bands (about 0.7%). Of these, two had matches in Gene Bank: one was MCH (Fig. 1) and the other was the mouse oncogene, *fau*. A third band had homology to a DNA-binding factor, and three additional bands that were differentially expressed had no known homology. Although the difference in MCH expression on differential displays appeared to be absolute, that is, no signal was detected in the *ob/+* mice versus an obvious signal in *ob/ob* mice, assessment of MCH expression using a ribonuclease protection assay showed that the difference between fed *ob/ob* and *ob/+* mice was a 50–80% increase in the *ob/ob* animal (Fig. 1b).

To evaluate further the expression of MCH in lean versus obese mice and to evaluate the possibility that MCH expression was affected by nutritional status, C57Bl/6J mice *+/+*, C57Bl/6J *ob/+* heterozygotes and C57Bl/6J *ob/ob* animals were compared both in the fed state and after 24 hours of fasting. In these experiments we also probed for neuropeptide Y (NPY) mRNA because it is known that NPY expression increases with fasting and is also increased in *ob/ob* mice. Figure 2 shows the results of hypothalamic mRNA blots in fed and fasted mice probed for MCH or NPY. In the fed state, wild-type control mice express low levels of MCH, whereas *ob/+* animals and *ob/ob* animals express higher levels of MCH. Fasting led to an increase in MCH expression in all three groups of animals.

Figure 3 shows the quantitative data derived from several experiments. Figure 3a and b compares relative expression of MCH in the fed and fasted state in control, heterozygous and

† Present address: Department of Clinical Chemistry, Glostrup Hospital, University of Copenhagen Medical School, DK2600 Glostrup, Denmark.

|| To whom correspondence should be addressed.